Materials Chemistry and Physics 225 (2019) 239–246

Contents lists available at ScienceDirect

Materials Chemistry and Physics

journal homepage: www.elsevier.com/locate/matchemphys

Evaluation of mechanical and thermal properties of modified epoxy resin by using acacia catechu particles

Ahmer Hussain Shah[a,b], Xiao Li[a], Xiaodong Xu[a,*], Abdul Qadeer Dayo[a,c], Wen-bin Liu[a], Jianwei Bai[a], Jun Wang[a]

[a] Key Laboratory of Superlight Material and Surface Technology, Ministry of Education, College of Materials Science and Chemical Engineering, Harbin Engineering University, Harbin, 150001, China
[b] Department of Textile Engineering, Balochistan University of Information Technology, Engineering and Management Sciences, Quetta, 87300, Pakistan
[c] Department of Chemical Engineering, Balochistan University of Information Technology, Engineering and Management Sciences, Quetta, 87300, Pakistan

HIGHLIGHTS

- Epoxy resin was modified by using the acacia catechu (AC) particles.
- FTIR analysis evidenced the progress of chemical reaction between particles and matrix.
- The composites have high flexural stress and bending strain.
- Shear banding phenomena and plasticization also increases impact strength.
- TGA showed improved thermal stability on increasing the AC amount.

ARTICLE INFO

Keywords:
Acacia catechu
Epoxy composites
Mechanical properties
Toughness
Thermal properties

ABSTRACT

In the current study, the epoxy/amine system is reinforced by the biodegradable Acacia Catechu (AC) particles on 0.5, 1.0, 1.5 and 2.0 wt (wt.) %. The AC/epoxy composites were characterized by Fourier transform infrared (FTIR) spectroscopy, thermogravimetric analysis (TGA), differential scanning calorimetry (DSC), dynamic mechanical analysis (DMA), scanning electron microscope (SEM), and mechanical properties. The increased hydrogen bonding for the AC/epoxy composites was observed by FTIR spectroscopy and DSC study confirmed the improved conversion of epoxy after the AC particles addition. 14% increase in the flexural strength and 94% improved impact strength were recorded on only 1.0 wt. % AC addition due to change in morphology and crosslink density. Moreover, slightly improved thermal stabilities were also recorded due to the aromatic tannin phenol structures of AC particles. The glass transition temperature values for AC/epoxy composites were observed at 143 and 148 °C by DSC and DMA, respectively; the decline in the values can be dedicated to the flexible segment of AC particles. The SEM analysis demonstrated shear banding phenomena between particles and matrix.

1. Introduction

The disposal of high performance polymers after use has produced negative effects on the environment; the biobased material reinforced polymer matrices can play a vital role in the development of the sustainable environment. The biodegradable materials are successfully reinforced in thermosets and thermoplastics matrices. The properties of polymeric matrices are modified by reinforcing the several biobased materials such as wood [1], cellulose [2], jute [3], corn husk [4], hemp [5,6], walnut shell [7], rice husk [8], kenaf [9], oil palm empty fruit bunch [10], and egg shell particles [11], both at micro and nano scale. The biobased fillers bring considerable advantages as compared to the artificial fillers, such as ceramics, glass and carbon fibres; advantages include renewable, easily available, eco-friendly, possess high specific strength, cheap, lighter, and easy to process [12–14].

Acacia catechu (AC), *er cha* in Chinese, is a polyphenol-based red tea, having catechin and epicatechin flavanol monomers, which can be converted into the hydrolyzable and condensed tannins *via* heat, acid catalyzed polymerization, cyclization of benzene and oxidative polymerization [15–18]. Moreover, tannins showed excellent anti-

* Corresponding author.
E-mail address: xuxiaodong@hrbeu.edu.cn (X. Xu).

https://doi.org/10.1016/j.matchemphys.2018.12.063
Received 26 June 2018; Received in revised form 12 December 2018; Accepted 23 December 2018
0254-0584/

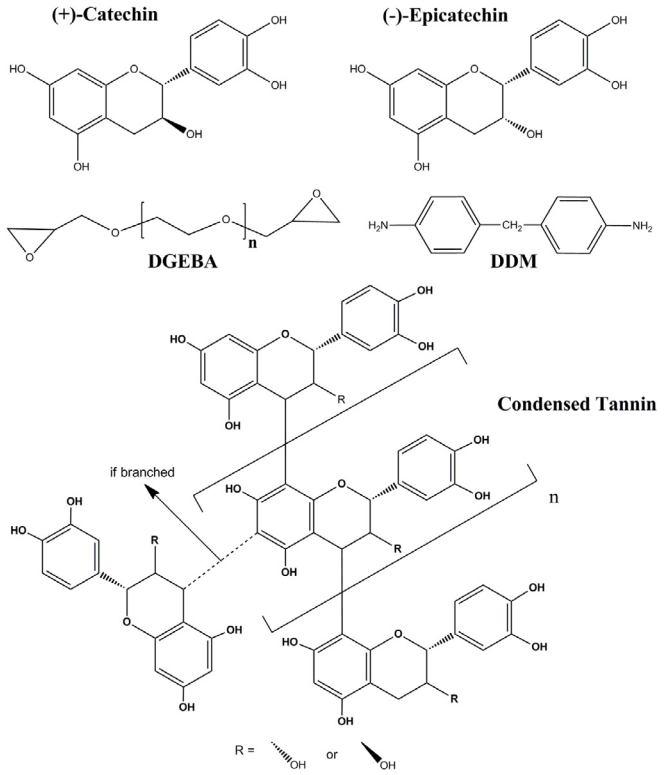

Scheme 1. Chemical structures of epoxy, DDM, catechin, epicatechin, and tannin.

inflammatory and anti-cancer activities [19], and AC extract has been used as a natural dye for wool [20], silk and cotton fabrics [21]. The addition of polyphenols extracted from green tea improved the mechanical and thermal properties of composites [22]. Recently, the tannic acid was used to reduce the brittleness of epoxy; simultaneously, improved the toughness and impact properties [23,24]. The polyphenols based extracts and the tannic acid improved the performance of matrices, it is obvious that the similar constituents having AC particles will have some favourable effects. The AC is a cheap and biodegradable material. Furthermore, the dispersion of particles plays an important role and affects the final morphology, common methods for improved particles dispersion are sonication [25,26], magnetic fields [27] and surfactant applications [28,29].

In the current study, the AC particles were loaded in the commercial epoxy, diglycidylether of bisphenol-A (DGEBA, E-51), cured with 4,4 diaminodiphenylmethane (DDM), structures are shown in Scheme 1. The AC particles were dispersed in epoxy by the mechanical stirring followed by ultrasonication without using any solvent. The blend was cured by using DDM as hardener at a 4:1 stoichiometric amount. The blends and cured composites were characterized by Fourier transform infrared (FTIR) spectroscopy, differential scanning calorimetry (DSC), dynamic mechanical analysis (DMA), thermogravimetric analysis (TGA), scanning electron microscope (SEM), flexural and impact studies, and results were compared with pristine epoxy/amine system.

2. Experimental

2.1. Materials

Commercial epoxy E-51 (1.56 g/cm^3 density and 184–195 g/mol epoxy equivalent weight) was purchased from Feng Huang Co. Ltd. China. The DDM (99.5%) was procured from Energy Chemical Co. Ltd. China. The AC powder was purchased from the local market of Harbin, China. The AC particles were soaked for 6 h at room temperature in a 0.5 wt. % NaOH solution to remove impurities, gums, and pectin. Later, the soaked particles were filtered and washed with ethanol and water until the complete neutralization and removal of residual NaOH. The obtained particles were overnight dried at 80 °C to remove the external water. The dried particles were ground via a ball-milled using a planetary ball mill (Pulverisette 7, FRITSCH) in a ZrO_2 vessel at a speed of 400 rpm for 4 h. The ball-to-powder weight ratio was kept as 15:1. The obtained samples were sieved with a standard sieve size of number 500 mesh and stored in airtight jars.

2.2. Preparation of the composites

The E51 matrix was taken in a glass beaker and heated at 80 °C; the desired mass of AC powder was added with filler loadings of 0.5, 1.0, 1.5, and 2.0 wt (wt.) %. The blend was stirred vigorously by a mechanical mixer at 300 rpm for 2 h at 80 °C. Afterwards, the blend was subjected to ultrasonication for 30 min to have the better dispersion of particles in the resin. Thereafter, the stoichiometric amount of hardener was added in the solution and stirred for a further 30 min to make it completely soluble in the solution. The mixture blend was poured into the moulds having the desired testing sample dimension and degassed in a vacuum oven at 80 °C for 30 min to evaporate any entrapped gases and to avoid air bubbles in the final cured samples which negatively influence on the performance. Later the specimens were cured in an air circulating oven as per the following sequence; 80 °C for 2 h and 140 °C for 3 h. This procedure was selected as epoxy synthesized by catechin can be cured at 150 °C without any degradation effects [30]. After curing the samples were surface polished from all sides to remove settled particles, if any. The blends and composites showed the increased depth of colour as the loading of AC wt % increased; this confirms better dispersion of AC particles in the matrix.

2.3. Characterizations

The AC particles size was calculated after the milling process by using a Malvern ZETASIZER nano series, UK, and SEM (CamScan MX 2600FE, Oxford Instruments, UK) at 20 kV.

The chemical structures of pristine, blends, and AC filled composites were studied by FTIR spectroscopy on a Perkin Elmer Spectrum 100 spectrometer, USA, which was equipped with a deuterated triglycine sulfate (DTGS) detector and KBr optics. The FTIR spectra were obtained in the range of 4000–400 cm^{-1} at 4 cm^{-1} resolution after averaging four scans by casting a KBr plate film. Two to three drops of neat or blend were taken on pristine KBr plate film and tested. For cured samples, a 2–3 mg sample powder was manually mixed with KBr and palate was formed by pressing and immediately tested.

The three-point bending test of the 3.2 × 12.7 × 125 mm^3 specimen was performed at room temperature 22 ± 2 °C according to ASTM D790 standard at 1 mm/min speed and 30.0 kN load cell capacity on a Universal Instron 4467, USA. A mean value of 10 samples for the same composition was produced as a result.

The impact assessment of the specimen was done by the Izod impact test on Tinius-Olsen impact-resistance device, USA, in accordance with ASTM D256-2010. The five test specimens of 63.5 × 12.7 × 3.2 mm^3 dimensions and a notch at 45° radius were tested for single composition, and mean value of the absorbed energy was reported.

The TGA was performed on a TA Instruments Q50, USA, at a heating rate of 20 °C/min from 40 to 800 °C under a 50 ml/min nitrogen flow rate. The DSC measurements were performed on a differential scanning calorimeter model TA Q200, TA Instruments, USA, under 50 ml/min flow of nitrogen. 5 mg of sample was weighed into a sample pan and tested immediately. The experiments were ranged from 30 to 230 °C at 20 °C/min heating rate.

The MetraviB DMA +450 was used to characterize the dynamic mechanical properties in a bending mode. The 35 × 10 × 3 mm^3 dimension samples were investigated at 1 Hz frequency from −50 to

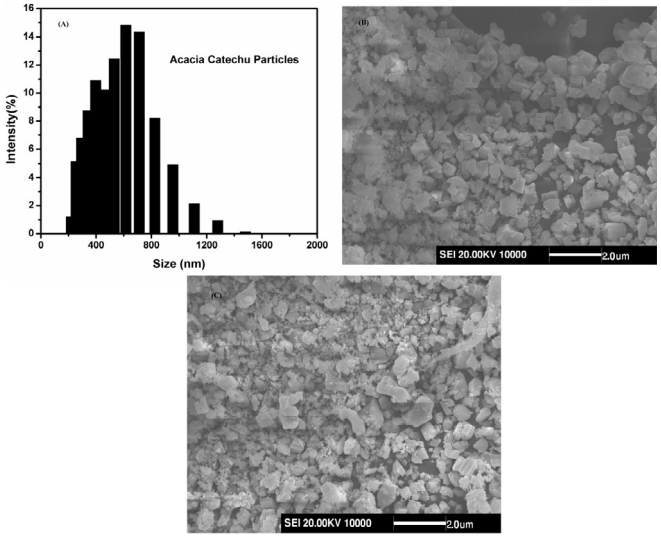

Fig. 1. Size distribution of AC particles.

250 °C with a heating ramp of 3 °C/min.

The surface morphologies of particles, pure epoxy, and their composites were investigated via SEM (CamScan MX 2600FE, Oxford Instruments, UK) at 20 kV. The flexural test fracture samples were collected carefully and sealed in polyethene bags for the SEM studies.

3. Results and discussion

3.1. Size determination

The size of AC particles was estimated after dispersing them in water at 25 °C and testing the solution on a Malvern ZETASIZER nano series. As shown in Fig. 1(A), the particle sizes from 260 to 1500 nm with several intensities were present. The calculated area of the plot showed that 88.6% of AC particles were in the nanometre range, while the remaining 11.4% were μm particles in 1–1.5 μm range. This confirms the average particles size was < 1 μm. Results were also verified by using the SEM analysis, the obtained micrographs depicted as Fig. 1(Band C) confirmed that majority of the particles were less than 1 μm size.

3.2. FTIR spectroscopy studies

The FTIR spectroscopy studies were conducted to detect the changes in the structure of monomer, blends and polymers and plotted in Fig. 2. The characteristics band located at 910 cm^{-1} corresponds to C–O stretching of oxirane group, a decline of this band reflects curing of the epoxy resin. The –OH stretching vibrations were located at 3550 and 3409 cm^{-1}. The region 2900–2800 cm^{-1} corresponds to saturated C–H stretching vibrations and the peak located at 3034 cm^{-1} corresponds to unsaturated = C–H stretching vibrations. The characteristics peak at 1608 and 1509 cm^{-1} correspond to C = C and C–C of aromatic benzene rings while 1036 cm^{-1} corresponds to C–O–C stretching vibrations of ethers. The structure of monomer depicted in Fig. 2(A) represents, for instance, the peak positions and intensities at 3056, 1430, 1345, and 1132 cm^{-1} have changed after blending the AC particles with the matrix. These changes suggest the reaction between particles and matrix, however, the intensity of the mentioned peaks is less and overlapping with other peaks cannot give accurate quantification [31]. Furthermore, the –OH stretching peak intensity at 3401 cm^{-1} of pristine epoxy decreases and shifts to 3518 cm^{-1} for the epoxy/AC blend sample, this suggests that the particles take part in the polymerization reaction of epoxy and attached to the epoxy backbone. Moreover, a broader absorbance peak for –OH (3500 cm^{-1}) was observed due to AC

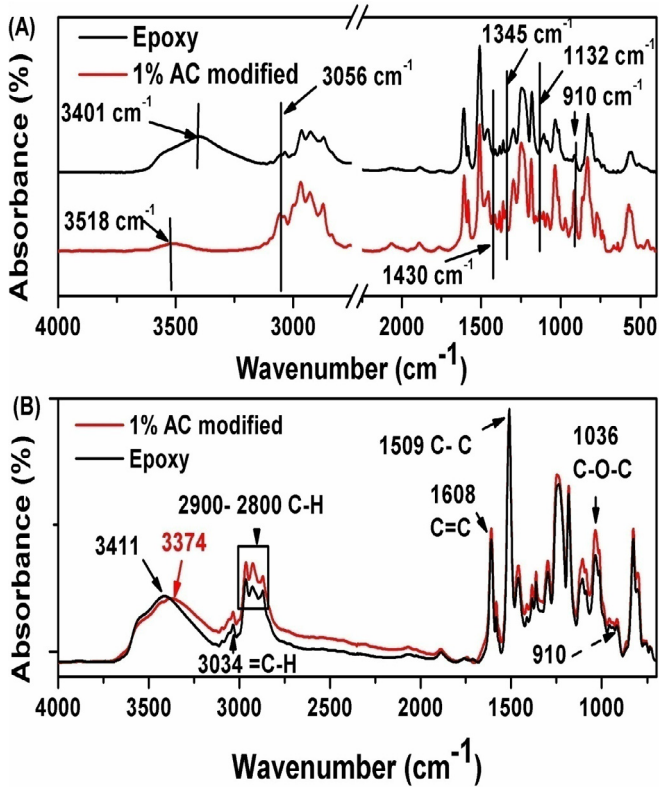

Fig. 2. FTIR of neat epoxy monomer and 1.0 wt% AC modified epoxy blend (A), cured neat epoxy and 1.0 wt% AC modified epoxy (B).

particles containing the –OH groups. The FTIR spectra of cured structures depicted in Fig. 2(B) shows the increasing peak intensity near 1100 cm^{-1}, corresponding to C–N bonds with some ether. The AC modified sample showed increased intensity of this peak, which represents the accelerated curing process in the presence of AC particles. The epoxide ring opening process is usually observed by the increasing peak of –OH stretching, at around 3500 cm^{-1}. It is well known that the shifting of –OH characteristics peak from higher to lower wave number represents increased hydrogen bonding in the network [32–34]. From Fig. 2(B), we can easily observe the shifting of –OH peak from 3411 to 3374 cm^{-1} for pristine epoxy and AC filled epoxy, in addition to this, a slight deflection in the region of 3575 to 3430 cm^{-1} [35,36]. These observations confirm the intermolecular and/or intramolecular hydrogen bonding between AC particles and epoxy matrix. The curing process reaction was catalyzed by the additional –OH groups from the AC particles and the AC particles were attached to the epoxy backbone [37,38]. The possible reaction mechanisms involved for the epoxy/AC particles system based on the above observations are shown in Scheme 2, Scheme 3 and Scheme 4.

3.3. Differential scanning calorimetry of AC/epoxy blends

The influence of AC particles introduction on the curing behaviour of the epoxy/amine system was studied. Fig. 3(A) shows the DSC exothermic curves of neat epoxy/amine and epoxy/amine resins with different AC wt. % loadings. The DSC data for peak temperature and total enthalpy of curing are summarized in Table 1.

It can be seen that all the AC modified blends lower the exothermic peaks and onset temperatures in comparison to the pristine epoxy/amine system. The onset temperatures and exothermic peaks were decreased by increasing the amount of AC from 0 to 1.5 wt. % and were recorded as 110, 102, 94, 90 °C and 180, 174, 169, and 168 °C respectively. This drop in temperature confirms the catalytic effect of –OH groups (tannins) of AC in blends. The results also indicate that an

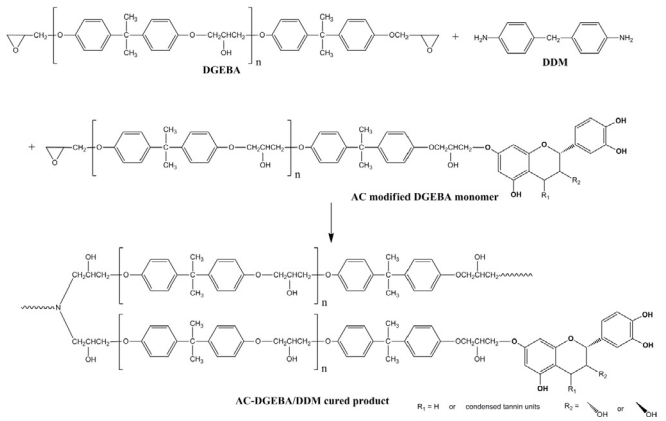

Scheme 2. Possible reaction mechanism of AC with the epoxy/amine system.

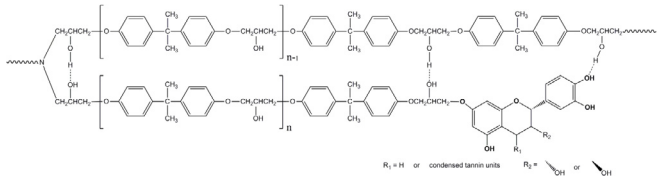

Scheme 3. Intramolecular hydrogen bonding between epoxy and AC particles.

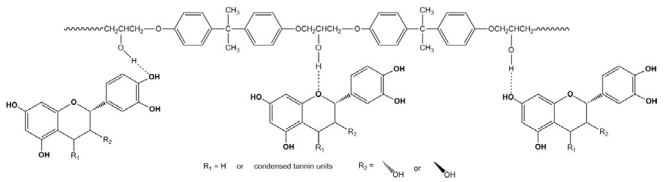

Scheme 4. Intermolecular hydrogen bonding between epoxy and AC particles.

increase in AC particles decreases the heat of polymerization (ΔH) and the exothermic peak heights for all the blends. The highest value of the exothermic peak was observed at 180 °C for the neat epoxy/amine system, while the lowest value was recorded at 168 °C for AC 1.5 wt. % loading. The ΔH was recorded in the range from 383 to 295 J/g for pristine and 1.0 wt. % AC content blends, respectively. The ΔH value slightly increases on the loading of 1.5 wt. % AC particles in the blend. This behaviour indicates that the particles of AC are taking part in or catalyzing the cure reaction and the maximum amount is limited to 1.0 wt. %, beyond this, the particles need more energy to take part in the reaction mechanism.

In addition to this, the conversion plot (Fig. 3(B)) also showed that only 1.0 wt. % AC particles addition increase the conversion at a given temperature. The AC particles having tannins are responsible for this behaviour, additionally, the –OH groups of tannins catalyzes the cure reaction of thermosets [39,40].

3.4. Thermomechanical analysis

The effect of AC loading in epoxy was studied by dynamic mechanical thermal properties which measure important parameters, storage modulus (E'), loss modulus, damping factor ($tan\ \delta$), glass transition temperature (T_g) and β - relaxation temperature (T_β). The results are produced in Fig. 4 and summarized in Table 2.

The damping factor is an important function for the high performance polymer composites, both β and α transition (T_β and T_α) were observed, peak in lower temperature region is T_β, while the peak observed in higher temperature region is T_α, which is also known as T_g. The intensity transition at low temperature (−50 to 0 °C), corresponds to the motion of side chain or neighbour molecules of the main chain

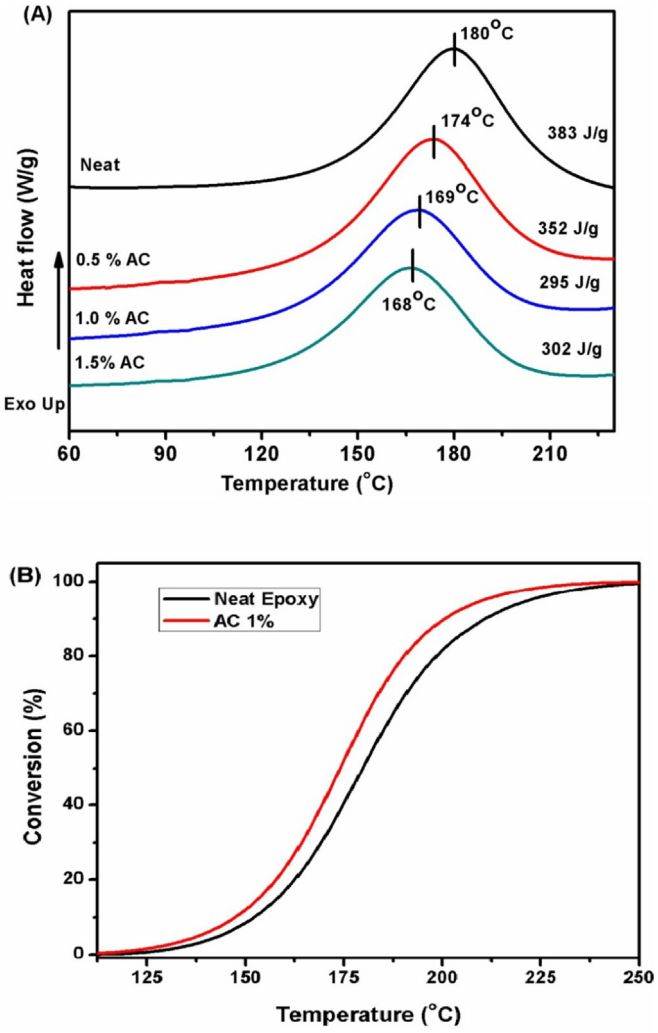

Fig. 3. DSC thermogram for neat and AC modified epoxy monomers (A), and conversion plot of neat and 1.0 wt. % AC epoxy against the temperature (B).

Table 1
DSC parameters of neat resin and AC blends at different content.

Sample	Initial exotherm (°C)	Peak exotherm (°C)	Heat of reaction (J/g)
Neat	110	180	383
0.5% AC	102	174	352
1.0% AC	94	169	295
1.5% AC	90	168	302

[41]. The T_β value continues to rise as the amount of AC increases; this confirms the increased intermolecular hydrogen bonding. The enhancement of β-transition magnitude can be related to increased torsional vibration of side chains due to increased hydrogen bonding, resulting in improvement in toughness, even when the crosslink decreases as calculated from Eq (1). A 0.27×10^{-3} mol/cm^3 decline in the covalent crosslink and an improvement of 0.016 in the β-transition peak value was observed till 1.0 wt. % AC loading. However, on further addition of AC particles, a sharp decline (0.95×10^{-3} mol/cm^3) in the covalent crosslink and a slightly increased (0.01) β-transition values were observed. This sharp decline in the covalent crosslink after 1.0 wt. % AC loading will bring negative impacts on the mechanical properties, as will be discussed later.

A decreasing trend was observed for T_g as the loading of AC particles in epoxy/amine system was increased. In addition to this, slightly higher $tan\ \delta$ peaks for AC modified epoxies were also observed; this

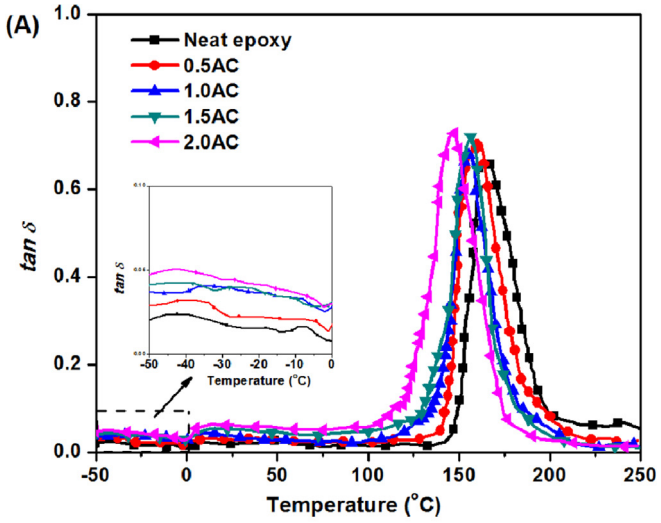

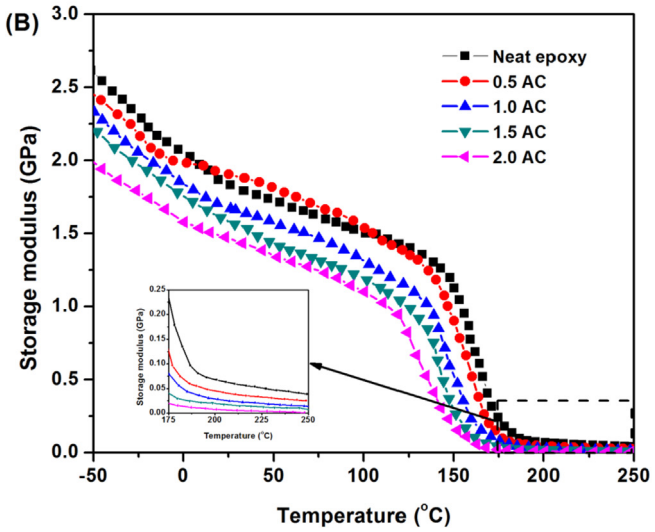

Fig. 4. *tan δ* (A) and storage modulus (B) values against temperature.

Table 2
Glass transition temperatures and cross-link densities of neat resin and AC filled composites.

Sample	*tan δ* peak height at −50°C (T_β)	T_g (°C)		Cross-link density ($\times 10^{-3}$ mol/cm^3)
		DSC	*DMA*	
Neat	0.021	–	165	3.221
0.5% AC	0.028	154	161	3.101
1.0% AC	0.037	146	156	2.955
1.5% AC	0.041	145	155	2.378
2.0% AC	0.047	143	147	2.006

suggests the increased segmental movement of chains. This behaviour indicates the increase in loss factor, which means the energy dissipating capacity of the composites increased [42,43].

On the other hand, the stiffness (storage modulus at 50 °C) plotted as Fig. 4(B) also showed the decreasing trend as the amount of AC increased in the composites, similar behaviour was observed for the AC composites in the rubbery plateau region. The corresponding crosslink density was calculated by using the following equation and already illustrated in Table 2.

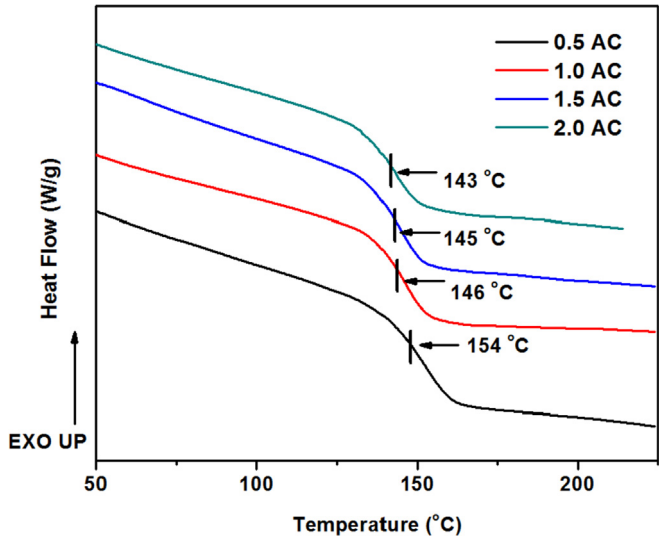

Fig. 5. DSC thermogram of AC modified cured samples.

$$\rho = \frac{E'}{3RT} \quad (1)$$

where ρ is the crosslink density (mol/cm^3), E' is the storage modulus in the rubbery plateau in MPa, R is the universal gas constant (8.3145 J/K mol), and T is the temperature at T_g + 50 in the rubbery plateau in Kelvin.

The decreasing T_g of AC containing epoxy composites confirms the decrease of crosslink densities in the rubbery plateau region. Therefore, the intermolecular motion and segment mobility take place easily, this improved the toughness. Moreover, the *tan δ* peaks show slight broadening in the onset and end set temperature (peak) region. The calculated crosslink densities of the pristine epoxy and epoxies reinforced AC showed a slight decline in the density values till 1.0 wt. % AC loading. Later, the crosslink densities values sharply decrease, which ultimately decrease the toughness of composites.

Furthermore, the T_g of AC filled epoxy composites was confirmed by the DSC analysis of cured samples, produced DSC curves are plotted as Fig. 5, while T_g values are reported in Table 2. The addition of AC particles in epoxy/amine system produces significant changes on the T_g values, as tannins of AC particles were miscible with epoxy. This can be attributed to the boundless compatibility between the components.

3.5. Mechanical properties

The stress-strain curves, obtained from three-point bending tests are depicted as Fig. 6 and the results are tabulated in Table 3. The flexural strength increase to 1.0 wt. % reinforcement of AC particles, the value reached to 139.9 ± 2.47 MPa, which is 14.9% higher than the neat epoxy 121.7 ± 2.31 MPa. Further addition of AC decreases the flexural strength and the value recorded as 131.8 ± 3.17 MPa on 2.0 wt. % AC loading. On the other hand, the flexural modulus of composites decreases on the addition of AC particles, which is almost the case with toughening systems for epoxies. It is interesting to note here, that the maximum decrease of modulus is 0.22 GPa on the 2.0 wt. % AC loading, which showed 8.7% decrease in the modulus of pristine epoxy recorded as 2.51 ± 0.027 GPa. These results confirmed that the loading of AC particles has affected the intermolecular chain mobility of the epoxy as discussed earlier in the thermomechanical section.

Moreover, the area under the flexural stress-strain curve (toughness) was calculated from all tested samples results of the neat matrix and AC containing composites; mean values with standard deviation are already tabulated in Table 3. A value of 3.46 ± 0.18 MPa was recorded for neat epoxy, while an increase of 24.8% and 53% was observed for

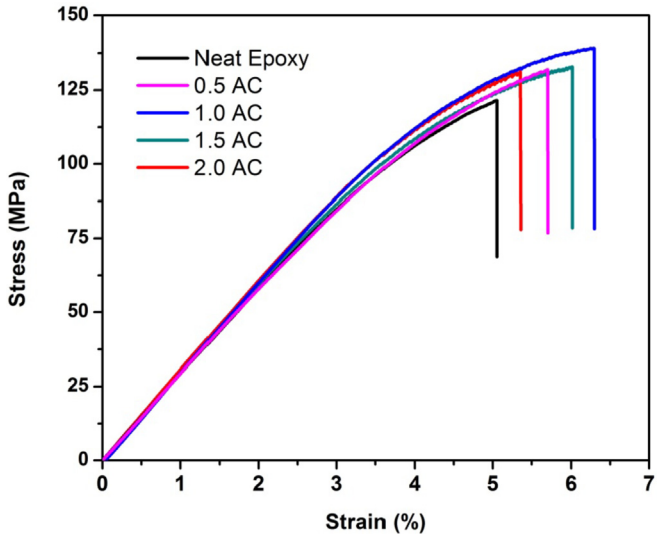

Fig. 6. Flexural stress and strain behaviour of neat epoxy and AC modified epoxy at different content.

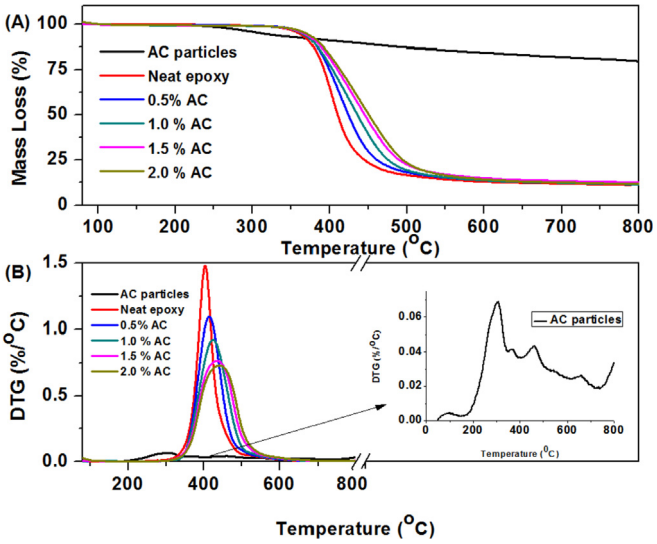

Fig. 7. Thermogravimetric analysis (A) and DTG (B) of AC particles, neat epoxy and AC modified epoxy at different content.

Table 3
Flexural, toughness and impact strength parameters for neat epoxy resin and AC modified blends.

Sample	Flexural strength (MPa)	Flexural modulus (GPa)	Toughness[a] (MPa)	Impact strength (kJ/m^2)
Neat	121.7 ± 2.31	2.51 ± 0.027	3.46 ± 0.18	11.05 ± 0.94
0.5%AC	132.1 ± 2.15	2.41 ± 0.025	4.32 ± 0.11	18.29 ± 2.27
1.0%AC	139.9 ± 2.47	2.35 ± 0.028	5.29 ± 0.14	21.46 ± 2.36
1.5%AC	132.4 ± 2.97	2.31 ± 0.025	4.76 ± 0.12	19.27 ± 2.91
2.0%AC	131.8 ± 3.17	2.29 ± 0.029	4.02 ± 0.17	16.89 ± 2.56

[a] Area under the stress-strain curve.

0.5 and 1.0 wt. % AC modified blends i.e. 4.32 ± 0.11 and 5.29 ± 0.14 MPa, respectively. The toughness of composites has a direct relationship with the filler distribution. If the AC particle distribution was not homogeneous in the matrix, a decline will be observed in the toughness. Results confirmed that the toughness of the epoxy/amine system was enhanced after the particles reinforcement.

Furthermore, the impact strengths were estimated by Izod impact tests, results are already reported in Table 3. As expected, the impact strength values continue to rise as the amount of AC particles increases in the epoxy network till 1.0 wt. %. The effect can be related to the two-phase nature of the system [44] and reduced cross-linking densities along with sufficient hydrogen bonding as evident in increased height of β - relaxation temperature. The impact strength for pristine epoxy/amine system was observed as 11.05 ± 0.94 kJ/m^2; the maximum improvement (94.2%) was recorded for 1.0 wt. % AC filled composite and value was read as 21.46 ± 2.36 kJ/m^2. Approximately similar values were recorded for 1.0 and 1.5 wt. % AC loading composites. The continuous increase in β - relaxation temperature height of 1.5 wt. % and 2.0 wt. % AC filled composites increases flexible segment and hence reduces the covalent cross-links to a greater extent which ultimately result in decreases in impact strength a little but the values are still higher than the pristine epoxy/amine system. The well-bound phases in the matrix can effectively transfer the applied load due to the strong hydrogen bonding between two phases [45]. The good dispersion of particles along with hydrogen bonding and strength effects the transfer of load; decreased homogeneity will reduce the strength but here the effect is compensated may be due to the formation of –OH groups in the structure distributed as a secondary network [46] which may also enhance the stress transfer from resin to the particles covered by bonds [47]. The improved toughness by incorporation of phenol derivatives in epoxy is also reported in the literature [48]. The AC particles phase dispersed within the network increased the chain mobility [49], and show the plasticizing effect which accounts for the improvement in toughness [23].

3.6. Thermal stabilities analysis

The thermal stability of the filler is an important function for the formation of composites. The high-performance thermosets have high curing temperatures around 150 to 250 °C. Generally, all bio fillers have lower thermal stability in this range which restricts the use of such fillers in high-temperature processing conditions [8].

The TGA and DTG curves under a nitrogen atmosphere from 50 to 800 °C for neat AC particles and epoxy resin, and composites with different AC wt. % are illustrated in Fig. 7 and corresponding thermal stability parameters are summarized in Table 4.

AC is a biobased filler having very good thermal stability as shown in Fig. 7(A), the 5% and 10% weight loss temperatures ($T_{5\%}$, $T_{10\%}$) and char yield at 800 °C (Y_c) were recorded as 311 °C, 428 °C and 81.9%, respectively; while DTG peak was observed at 305 °C as shown in Fig. 7(B). This confirms that AC particles can be processed with high-performance thermosets. The decomposition of AC occurred in several steps, the first step was evaporation of moisture and volatile substances and observed up to 120 °C. The next step initiated from 170 °C and finished at 350 °C with a maximum degradation rate at 305 °C. This decomposition step can be dedicated to the several flavanoid species.

The neat epoxy and AC/epoxy composites showed a single step of decomposition. The AC/epoxy composites showed improved thermal stability as compared to the pure epoxy. This represents that the formed blends were homogenous and bonds breakage in the structure was

Table 4
TGA summary for neat epoxy, AC particles, and AC containing composites.

Sample	$T_{5\%}$ (°C)	$T_{10\%}$ (°C)	$T_{20\%}$ (°C)	$T_{50\%}$ (°C)	Y_c (%) at 800 °C	DTG peak (°C)
AC Powder	311	428	–	–	81.9	305
Neat	360	374	387	410	10.8	403
AC 0.5%	364	379	392	424	11.6	414
AC 1.0%	365	380	395	435	11.2	424
AC 1.5%	367	383	400	445	12.3	435
AC 2.0%	370	386	404	450	11.4	442

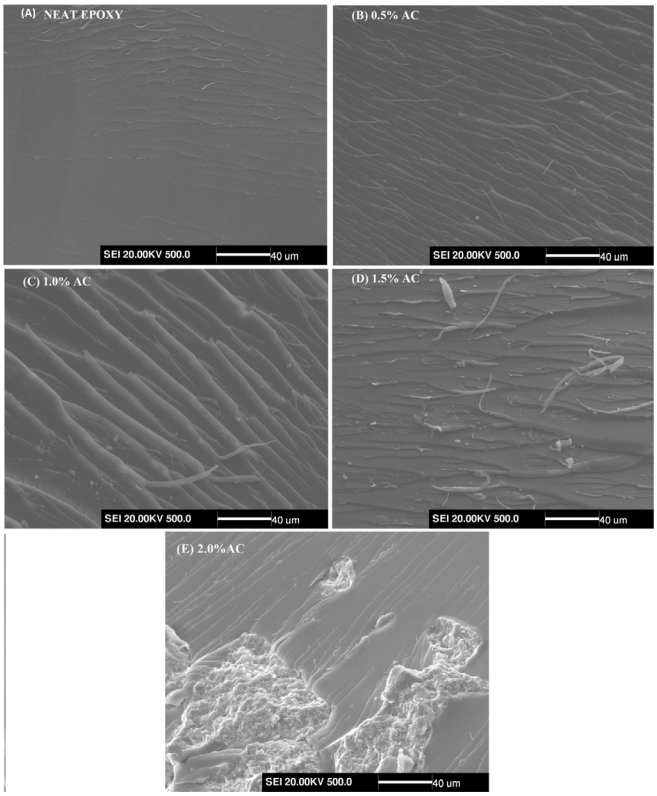

Fig. 8. SEM micrographs of fractured surfaces of neat epoxy (A), 0.5 (B) 1.0 (C), 1.5 (D), and 2.0 (E) wt. % AC modified epoxy.

concurrent. Considering the thermal stabilities behaviour of biobased filler, the decline in thermal stabilities was expected from the AC reinforcement. The AC filled epoxy composites showed slightly higher thermal stabilities values as compared to pristine sample, due to the better thermal stability of AC particles. The chemical crosslink of epoxy backbone with the phenolic structure of AC increases the thermal stabilities of the AC filled epoxy composites. The improved thermal stabilities also confirmed the formation of cross-links via hydrogen bonds. The aromaticity of formed compounds along with better adhesion of AC particles with epoxy results in the improved thermal behaviour of modified blends. Thermal stabilizes results confirmed that the AC/epoxy materials have better thermal stabilities at high temperatures in inert (nitrogen) atmospheres only.

3.7. SEM analysis

Fig. 8 presents the SEM micrographs of the flexural test fractured surfaces of neat epoxy and AC reinforced composites with different AC particles wt. % loading.

Fig. 8(A) shows the fracture surface of pristine epoxy, traditional smooth surface pattern epoxy fracture morphology was observed, which can be accounted as brittle having low toughness. The micrographs of AC modified samples, Fig. 8(B–E), reflects shear banding phenomena between epoxy and AC, which shows matrix shear yielding and plastic deformation over a large volume similar to rubber toughened epoxy systems. Cavities were not observed in all AC filled blends except 2 wt. % AC reinforced composites because of strong hydrogen bonding between particles and matrix. Initially, the particles were dispersed to form more miscible particle resin combination and on curing these small domains phase separated from the resin. The catechu particles have the ability to react themselves to form tannin resin molecules. For all modified blends, both flexibilization and toughening effects resulted in the maximum improvement in impact strength. The size of AC domains was relatively uniform and small for the lower content of AC Fig. 8(B and C). On the higher AC content (Fig. 8(D and E)) the homogeneity and dispersion decrease and AC agglomerate in the matrix were observed, which decrease the mechanical properties. For maximum enhancement in toughness, the phase distribution of AC particle along with strong interfacial adhesion by hydrogen bonding has primary importance. On the other hand, the agglomeration of small particles cannot act efficiently in dissipating mechanical energy but instead act as defects resulting in a decrease in toughness. Such a good interface interaction could efficiently transfer the stress between AC domains and epoxy matrix inducing plastic deformation and crack deflection. These morphological observations are in good agreement with the properties studied.

4. Conclusion

The effects of different AC particles wt. % loading on the curing and properties of the epoxy were successfully studied. The FTIR spectroscopy analysis of epoxy reinforced AC particles revealed chemical and hydrogen bonding cross-links in the composite. The DSC results revealed that AC particles accelerate the curing reaction of epoxy due to the tannin moieties of AC particles. Only 1.0 wt. % AC particles addition in epoxy improved the toughness and impact strength by 52% and 94%, respectively. On the higher loading of AC particles, the toughness and impact strength values were lower than the 1.0 wt. % AC particles, but the values are still higher than the corresponding values for the neat epoxy. AC filled epoxy composites also improved the thermal stability, the gradual rise was observed in all the thermal stabilities parameters, the degradation temperature peak was moved from 403 to 442 °C/min on only 2 wt. % AC particles reinforcement. The T_g values for 2 wt. % reinforced AC particles composites were observed at 143 and 148 °C by DSC and DMA, respectively. These values are slightly lower than the neat matrix values, this decline can be dedicated to the flexible chains of AC particles. Excellent phase distribution of AC particles was observed in SEM analysis, which reflects the shear yielding and plastic deformation over a large volume. The produced composite materials would be stable at high temperatures in inert atmospheres.

Acknowledgement

The authors acknowledge the financial support received from the National Natural Science Foundation of China (Project No. 21404027), the Open Research Fund of State Key Laboratory of Polymer Physics and Chemistry, Changchun Institute of Applied Chemistry, Chinese Academy of Sciences, and the Natural Science Foundation of Heilongjiang Province of China (No. QC2016060).

References

[1] E.O. Olakanmi, M.J. Strydom, Critical materials and processing challenges affecting the interface and functional performance of wood polymer composites (WPCs), Mater. Chem. Phys. 171 (2016) 290–302.
[2] A.K. Sevda Boran, Esra Erbas Kiziltas, Douglas J. Gardner, Characterization of ultrafine cellulose-filled high-density polyethylene composites prepared using different compounding methods, BioResources 11 (4) (2016) 8178–8199.
[3] J.M. Vijay Baheti, Reinforcement of wet milled jute nano/micro particles in polyvinyl alcohol films, Fibers Polym. 14 (1) (2013) 133–137.
[4] A.M. Youssef, A. El-Gendy, S. Kamel, Evaluation of corn husk fibers reinforced recycled low density polyethylene composites, Mater. Chem. Phys. 152 (2015) 26–33.
[5] Y.-l. Xu, et al., Mechanical and thermal properties of a room temperature curing epoxy resin and related hemp fibers reinforced composites using a novel in-situ generated curing agent, Mater. Chem. Phys. 203 (2018) 293–301.
[6] A.Q. Dayo, et al., The influence of different chemical treatments on the hemp fiber/polybenzoxazine based green composites: mechanical, thermal and water absorption properties, Mater. Chem. Phys. 217 (2018) 270–277.
[7] A.H. Shah, et al., Effect of alkali treated walnut shell (juglansregia) on high performance thermosets. Study of curing behavior, thermal and thermomechanical properties, Digest J. Nanomater. Biostructures 13 (3) (2018) 857–873.
[8] R.S. Chen, S. Ahmad, Mechanical performance and flame retardancy of rice husk/organoclay-reinforced blend of recycled plastics, Mater. Chem. Phys. 198 (2017) 57–65.
[9] P.-Y. Chen, et al., Preparation, characterization and crystallization kinetics of Kenaf

fiber/multi-walled carbon nanotube/polylactic acid (PLA) green composites, Mater. Chem. Phys. 196 (2017) 249–255.
[10] N. Saba, et al., Physical, structural and thermomechanical properties of oil palm nano filler/kenaf/epoxy hybrid nanocomposites, Mater. Chem. Phys. 184 (2016) 64–71.
[11] A.H. Shah, et al., Reinforcement of stearic acid treated egg shell particles in epoxy thermosets: structural, thermal, and mechanical characterization, Materials 11 (10) (2018).
[12] A.Q. Dayo, et al., Natural hemp fiber reinforced polybenzoxazine composites: curing behavior, mechanical and thermal properties, Compos. Sci. Technol. 144 (2017) 114–124.
[13] A. Zegaoui, et al., Influence of fiber volume fractions on the performances of alkali modified hemp fibers reinforced cyanate ester/benzoxazine blend composites, Mater. Chem. Phys. 213 (2018) 146–156.
[14] A. Zegaoui, et al., Tailoring the desired properties of dicyanate ester of bisphenol-A/bisphenol-A based benzoxazine resin by silane-modified acacia catechu particles, React. Funct. Polym. 131 (2018) 333–341.
[15] A.D.a.L. Avérous, Characterization and physicochemical properties of condensed tannins from Acacia catechu, J. Agric. Food Chem. 64 (2016) 1751–1760.
[16] Micucci Matteo, et al., Newer insights into the antidiarrheal effects of Acacia catechu willd. Extract in Guinea pig, J. Med. Food 20 (6) (2017) 592–600.
[17] A.A.a.L. Avérous, Chemical modification of tannins to elaborate aromatic biobased macromolecular architectures, Green Chem. 17 (2626) (2015) 2626–2646.
[18] P. Baruah, R. Duarah, N. Karak, Tannic acid-based tough hyperbranched epoxy thermoset as an advanced environmentally sustainable high-performing material, Iran. Polym. J. (Engl. Ed.) 25 (2016) 849–861.
[19] M.I. Khan, A. Ahmad, S.A. Khan, M. Yusuf, M. Shahid, N. Manzoor, Assessment of antimicrobial activity of catechu and its dyed substrate, Clean. Prod. 19 (12) (2011) 1385–1394.
[20] F.M. Mohd Yusuf, Mohd Shabbir, Mohd Ali Khan, Eco-dyeing of wool with Rubia cordifolia root extract: assessment of the effect of Acacia catechu as biomordant on color and fastness properties, Textil. Cloth. Sustain. 2 (10) (2016).
[21] S. Jose, H. Gurumallesh Prabu, L. Ammayappan, Eco-friendly dyeing of silk and cotton textiles using combination of three natural colorants, J. Nat. Fibers 14 (1) (2017) 40–49.
[22] H.X.,C.S.H. Xiang, Y.H. Cheng, Z. Zhou, M.F. Zhu, Structural characteristics and enhanced mechanical and thermal properties of full biodegradable tea polyphenol/poly(3-hydroxybutyrate-co-3-hydroxyvalerate) composite films, Express Polym. Lett. 7 (9) (2013) 778–786.
[23] Xiaoma Fei, Wei Wei, Fangqiao Zhao, Ye Zhu, Jing Luo, Mingqing Chen, Xiaoya Liu, Efficient toughening of epoxy-anhydride thermosets with a bio-based tannic acid derivative, ACS Sustain. Chem. Eng. 5 (1) (2017) 596–603.
[24] X. Fei, et al., Tannic acid as a bio-based modifier of epoxy/anhydride thermosets, Polymers 8 (9) (2016) 314.
[25] Y. Ma, et al., Porous lignin based poly (acrylic acid)/organo-montmorillonite nanocomposites: swelling behaviors and rapid removal of Pb (II) ions, Polymer 128 (Supplement C) (2017) 12–23.
[26] S. Jun, et al., Silane coupling agent modified BN–OH as reinforcing filler for epoxy nanocomposite, High Perform. Polym. 31 (1) (2019) 116–123.
[27] G. Ying, et al., Mechanical and dielectric properties of epoxy composites filled with hybrid aluminum particles with binary size distribution, High Perform. Polym. 31 (1) (2019) 124–134.
[28] T. Liu, et al., A graphene quantum dot decorated SrRuO3 mesoporous film as an efficient counter electrode for high-performance dye-sensitized solar cells, J. Mater. Chem. 5 (34) (2017) 17848–17855.
[29] Z. Sun, et al., Experimental and simulation-based understanding of morphology controlled barium titanate nanoparticles under co-adsorption of surfactants, CrystEngComm 19 (24) (2017) 3288–3298.
[30] M.O. Sunita Basnet, Chizuru Sasaki, Chikako Asada, Yoshitoshi Nakamura, Functionalization of the active ingredients of Japanese green tea (Camellia sinensis) for the synthesis of bio-based epoxy resin, Ind. Crop. Prod. 73 (2015) 63–72.
[31] S. Cholake, et al., Quantitative analysis of curing mechanisms of epoxy resin by mid- and near- fourier transform infra red spectroscopy, Def. Sci. J. 64 (3) (2014) 314–321.
[32] María González González, J.C.C.a.J.B., Applications of FTIR on epoxy resins – identification, monitoring the curing process, phase separation and water uptake, in Infrared Spectroscopy - Materials Science, Engineering and Technology. INTECH: Spain.
[33] Q.W. LIANG LI, L.I. SHANJUN, P.E.I.Y.I. WU, Study of the infrared spectral features of an epoxy curing mechanism, Appl. Spectrosc. 62 (10) (2008) 1129–1136.
[34] A.A.D.-S. Wei Zhang, Richard S. Blackburn, IR study on hydrogen bonding in epoxy resin–silica nanocomposites, Prog. Nat. Sci. 18 (2008) 801–805.
[35] D. Chmielewska, T. Sterzyński, B. Dudziec, Epoxy compositions cured with aluminosilsesquioxanes: thermomechanical properties, J. Appl. Polym. Sci. 131 (17) (2014).
[36] F. Fraga, et al., Curing kinetics of the epoxy system diglycidyl ether of bisphenol A/isophoronediamine by Fourier transform infrared spectroscopy, Polym. Adv. Technol. (2008).
[37] J. Baller, et al., The catalytic influence of alumina nanoparticles on epoxy curing, Thermochim. Acta 517 (1–2) (2011) 34–39.
[38] B.A. Rozenberg, Kinetics, thermodynamics and mechanism of reactions of epoxy oligomers with amines, in: K. Dušek (Ed.), Epoxy Resins and Composites II, Springer Berlin Heidelberg, Berlin, Heidelberg, 1986, pp. 113–165.
[39] J.-S. Fariba, M. Behrooz, B. Hossein, Effect of dendrimer-functionalized magnetic iron oxide nanoparticles on improving thermal and mechanical properties of DGEBA/IPD epoxy networks, High Perform. Polym. 31 (1) (2019) 24–31.
[40] A.Q. Dayo, et al., Reinforcement of economical and environment friendly Acacia catechu particles for the reduction of brittleness and curing temperature of polybenzoxazine thermosets, Compos. Appl. Sci. Manuf. 105 (2018) 258–264.
[41] R. Ghanbaralizadeh, et al., A novel method for toughening epoxy resin through CO_2 fixation reaction, J. CO_2 Util. 16 (2016) 225–235.
[42] H. Feng, X. Wang, D. Wu, Fabrication of spirocyclic phosphazene epoxy-based nanocomposites with graphene via exfoliation of graphite platelets and thermal curing for enhancement of mechanical and conductive properties, Ind. Eng. Chem. Res. 52 (30) (2013) 10160–10171.
[43] S. Ma, et al., Effect of solvents on the curing and properties of fully bio-based thermosets for coatings, J. Coating Technol. Res. 14 (2) (2017) 367–375.
[44] D.S. Shailesh kumar shukla, Blends of modified epoxy resin and carboxyl-terminated polybutadiene, J. Appl. Polym. Sci. 100 (3) (2006) 1802–1808.
[45] R.F. Landel, L.E. Nielsen, Mechanical Properties of Polymers and Composites, C. Press, 1993.
[46] R. Ghanbaralizadeh, H. Bouhendi, K. Kabiri, M. Vafayan, A novel method for toughening epoxy resin through CO_2 fixation reaction, J. CO_2 Util. 16 (2016) 225–235.
[47] C. Wang, et al., Silver nanoparticles/graphene oxide decorated carbon fiber synergistic reinforcement in epoxy-based composites, Polymer 131 (Supplement C) (2017) 263–271.
[48] W. Thielemans, R.P. Wool, Lignin esters for use in unsaturated thermosets: lignin modification and solubility modeling, Biomacromolecules 6 (2005) 1895–1905.
[49] M. Xiangsheng, et al., 2,3,3′,4′-Oxydiphthalic dianhydride-based phenylethynyl-terminated imide oligomers for low-temperature resin transfer molding applications, High Perform. Polym. 28 (8) (2015) 962–970.